Built Heritage

RESEARCH ARTICLE

Open Access

Types of lime binders in mortars used for the construction of the Ming Great Wall of China and their importance for the development of a conservation strategy

Tanja Dettmering[1,2*] and Shibing Dai[2]

Abstract

The most obvious characteristics of the Ming Great Wall are external masonry walls made of natural stones, bricks and lime mortars. According to the chemical and mineralogical compositions of the original bedding and pointing mortars, dolomitic lime binder was used dominantly in the construction of the Ming Great Wall in provinces such as those around Beijing and Hebei. Calcium-rich lime and air lime with low natural hydraulically reactive phases, which are hydrated and react slowly with the carbon dioxide in air to form calcium carbonate, were used in some western provinces. Chemical and microscopic investigations show that both dolomitic and calcium-rich lime mortars are almost aggregate-free. Historic dolomitic lime mortars are characterised by high strengths, low porosities and dense micro-scale textures. The most recent conservation principle is to preserve the Ming Great Wall as a ruin. Therefore, the conservation strategy should be redefined in terms of mortars. Since some of the damage to the Great Wall is related to reactions between dolomitic lime mortars and air pollutants, calcium-rich lime binders should be used for conservation and even for restoration of those parts of the Great Wall that were originally built with dolomitic lime. Binders based on natural hydraulic lime and calcium-rich lime gauged with natural pozzolana might be more compatible than other binders" for the structural consolidation of the ruins of the Great Wall.

Keywords: Great Wall, Masonry ruins, Lime mortars, Dolomitic lime, Deterioration, Conservation

1 Introduction

Many parts of the Ming Great Wall of China, built by the Ming dynasty, are in danger of decay. The reasons for this need to be carefully examined to find the best way to develop a preservation strategy. Different circumstances in the past have contributed to the current condition of the Wall, which is being examined as part of a larger study. According to the 2018 Master Plan guidelines, lime mortars used in the construction of masonry are a special feature of in situ conservation. It is necessary to study lime mortars in detail to understand their composition and to develop conservation materials that are as faithful as possible to the original materials and that deliver the best results under environmental conditions. The present article describes a preliminary study that describes mortars, including their characteristic dolomitic and calcitic lime binders with very low proportions of aggregates, in detail for the first time using traditional chemical-mineralogical methods in combination with new imaging techniques. Based on the history and construction methods of the Great Wall of China and current conservation philosophies, the research methods and results are presented as part of a larger study to characterise the original mortars at selected sites and samples. Notes are given on the physical and mechanical properties and

*Correspondence: tanja.dettmering@arcor.de
[2] Architectural Conservation Laboratory CAUP Tongji University, No. 1239 Siping Road, Shanghai 200092, China
Full list of author information is available at the end of the article

Springer Open

© The Author(s) 2022. **Open Access** This article is licensed under a Creative Commons Attribution 4.0 International License, which permits use, sharing, adaptation, distribution and reproduction in any medium or format, as long as you give appropriate credit to the original author(s) and the source, provide a link to the Creative Commons licence, and indicate if changes were made. The images or other third party material in this article are included in the article's Creative Commons licence, unless indicated otherwise in a credit line to the material. If material is not included in the article's Creative Commons licence and your intended use is not permitted by statutory regulation or exceeds the permitted use, you will need to obtain permission directly from the copyright holder. To view a copy of this licence, visit http://creativecommons.org/licenses/by/4.0/.

physico-chemical compatibility of magnesium-rich dolomitic lime mortars as a basis for the evaluation of original mortars and future design of repair mortars. These results and new findings are discussed to develop a conservation strategy based on compatible lime mortars.

2 The Great Wall of the Ming Dynasty

2.1 History and cultural significance

The Great Wall of China, declared to be a UNESCO World Heritage Site in 1987, is a network of fortifications built from the third century BC under Qin Shin Huang through the 17th century on the northern border of the country (to present-day Mongolia). The Great Wall became the largest military structure in the world (Luo et al. 1993). The Great Wall built by the Ming Dynasty, referred to as the Ming Great Wall, includes numerous watchtowers, signal towers, fortresses, garrisons, passes, gates, administrative cities, and supply stations and is the most famous part of the network of the Great Wall (Fig. 1).

Since the beginning of the 20th century, the Great Wall has been a symbol for all of China. On September 30, 2019, a plan was announced for a Great Wall Cultural Park that will bring history, architecture and landscape to life (Fig. 2).

2.2 Damage and conservation approaches

The Ming Great Wall has been damaged by both anthropogenic and natural influences (Fig. 3). The causes of damage were found to be defects at the time of construction, removal of stone and bricks for new construction and natural weathering. The damage seems to have accelerated over the last two decades.

Previous measures to preserve the Ming Wall have followed two philosophies (Fig. 4). Reconstruction was preferred, especially from the 1980s to the beginning of the 21st century. However, based on further research and the

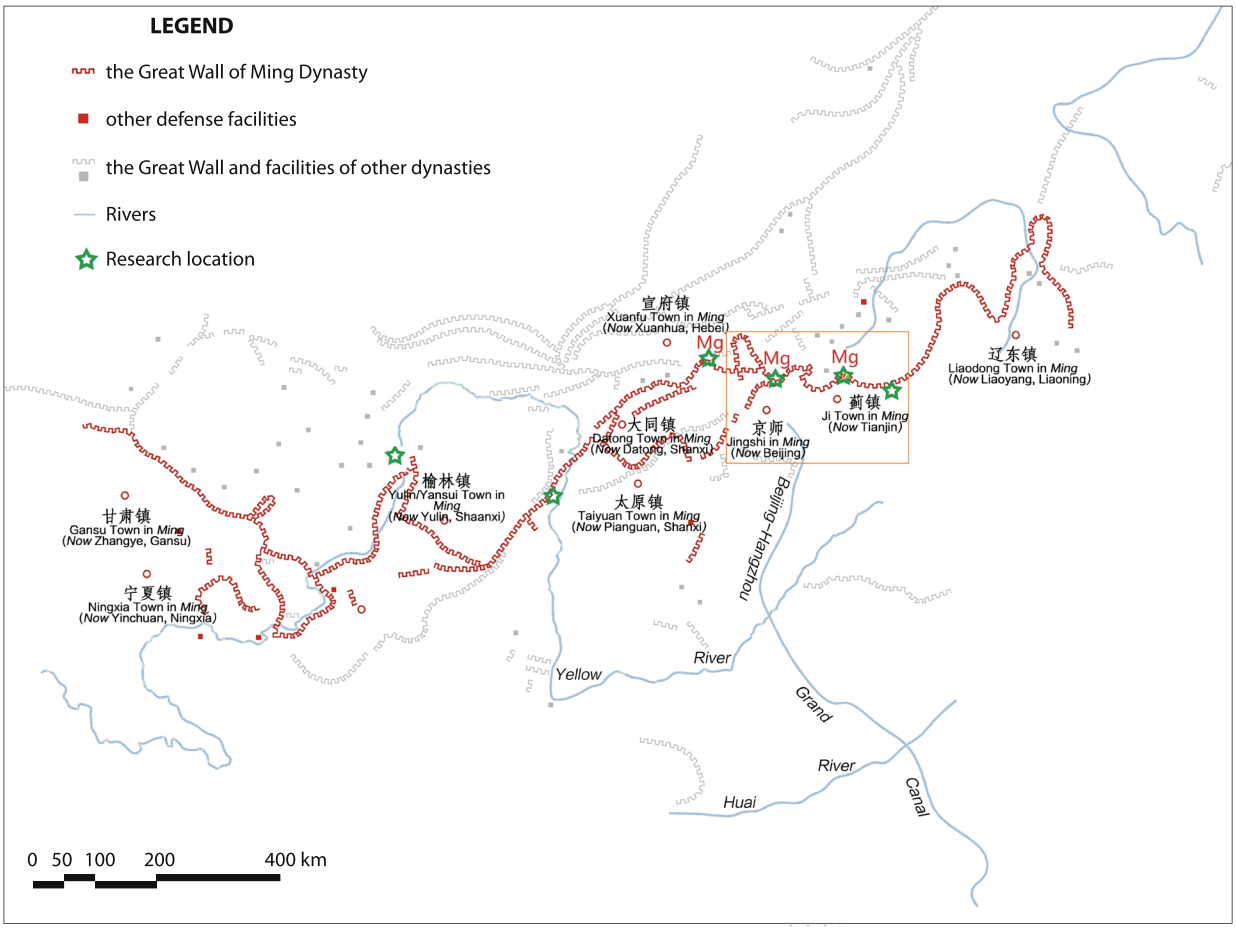

Fig. 1 Map of the Ming Great Wall with sampling points (green stars) and dolomitic lime binder (red "Mg"). The Ming Great Wall in the yellow square frame was built under the former Ji Town administration (Source: Tongji-ACL, revised based on Wang 2021)

Fig. 2 The unrestored Ming Great Wall is becoming part of the landscape (Source: Tongji-ACL, taken in Liaoning Province)

coexistence of ruins and architectural forms, the overall strategy of in situ conservation has been increasingly recognised and emphasised (WHC 2018, 2019; Wang 2021). "To conserve in situ completely and with little intervention and as close to the original (recreated) materials as possible," is the guideline of the 2018 Masterplan. Accordingly, the five guiding principles for conservation and restoration activities at the property (protection of the original state of the Great Wall, minimal intervention, preventive conservation, categorisation of heritage, and protection by grade according to the state of conservation) should be extended to all conservation and training activities.

Despite numerous restoration campaigns and reconstruction activities over the past four decades, parts of the Great Wall are still at risk of collapse, according to the State of Conservation Report of the World Heritage Committee (WHC 2018). Although building lime is prescribed for restoration (Fig. 5), lime mortars have not performed as well as historic mortars (Fig. 6). The guiding principle for conservation practice, according to Historic England publications (2008), is to use comparable materials in a "like for like" manner, i.e., to select suitable substitute materials that are as close as possible to the originals (Forster 2010).

2.3 Building materials and lime mortars used for the construction of the Ming Great Wall

The Ming Masonry Great Wall is the best preserved, most complete and most valuable part of the surviving

Fig. 3 Typical damage in Shanxi Province. Left: mainly anthropogenic. Right: mainly natural (Source: Tongji-ACL)

Fig. 4 Reconstruction (left) and conservation of ruins (right) in the capital city Beijing (Source: Tongji-ACL)

Fig. 5 Slaking and application of lime for restoration of the Ming Great Wall in 2019, Liaoning Province. **A** Slaking on site. **B** Preparation. **C** Bedding. **D** Grouting (Source: Tongji-ACL)

Fig. 6 No cracks were visible in historic pointing mortar based on dolomitic lime (left), while cracks were seen in new pointing mortars and at stone surfaces during recent restoration (right) (Source: Tongji-ACL)

Great Wall. Earth, natural stones and bricks were the primary materials used for construction, reconstruction and historic repair. Most of the walls were reconstructed from previous walls (Fig. 7).

The most frequently visited walls, e.g., those found in Beijing, are characterised by two walls, usually of brick, built on a stone foundation approximately six meters wide, and interior holes filled with various materials, such as rammed earth, stones, debris and mortars. The tops of the walls, as well as the outer walls, were made of bricks, and there was brick breastwork on two sides, so that the average total height was from six to eight meters (Fig. 8).

Most of the other parts of the wall were built with earth in the core, with or without stone-brick masonry (Fig. 9).

Fig. 7 An expansion of part of the Wall, Zhangjiakou, Hebei Province. Phase 1 (right): earthworks built before the Ming Dynasty from natural stonework without lime binder. Phase 2 (middle): natural stonework renewed at the beginning of the Ming Dynasty. Phase 3 (left): stonework built by the late Ming Dynasty. (Source: Tongji-ACL)

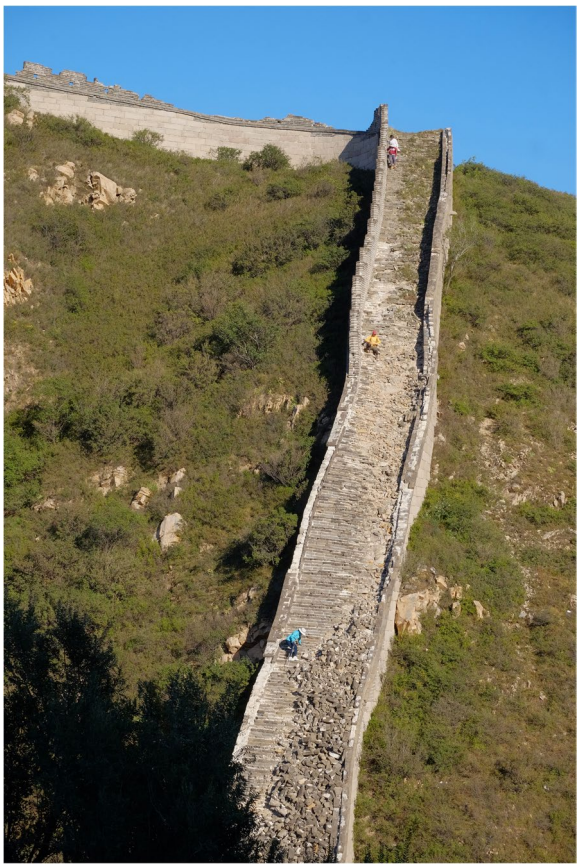

Fig. 8 A part of the Ming Great Wall in Beijing (before restoration in 2019), both sides of which were built with granite, brick and dolomitic lime mortars (Source: Tongji-ACL)

In western regions such as Shanxi and Gangsu, earth with plants was common in sites without brick masonry. Except for building lime, all materials were obtained locally.

Lime mortars were used for bedding, pointing or repointing stone and brick masonry (Fig. 10). Lime mortars were also used as grouts for filling voids in stone and brick masonry and gaps between earth and stone or brick. Lime was used for stabilising earth capping or pavement underneath the top of the Wall. Lime plasters and lime paints have survived on a few ruins of watchtowers. According to historical traditions, only "pure lime" without intentionally added aggregates was permitted for masonry construction (Figs. 11 and 12).

2.4 Previous and current studies of lime mortars

Traditional construction techniques are mentioned in historical literature of the Song and Qing dynasties in China (Dai 2018). However, there is no documentation of how lime was burned or processed for the construction of the Ming Great Wall because the construction of the Wall was a military operation.

Since 2008, two major national research projects on the "Scientific Study on Ancient Traditional Lime Mortars" have been conducted in China. The chemical composition and mineralogical components of a few lime mortar samples from the Ming Great Wall were analysed during the research; however, the results were not systematically studied. Research has focused on the addition of natural organic additives (Li et al. 2014; Yang, Zhang, and Ma 2010). To some extent, the properties of lime mortars under the influence of lime-rich mollusk shells and glutinous rice were investigated. Thus far, there have been no systematic studies of the lime binders in the mortars used in combination with stone and/or brick masonry and related damage to the Great Wall, as well as suitable restoration mortars.

Therefore, a current joint research project of the Academy for Heritage Architecture Research at Beijing University of Civil Engineering and Architecture in collaboration with the Architectural Conservation Laboratory of Tongji University (Tongji-ACL), Shanghai, has been initiated to understand traditional lime mortars and

Fig. 9 One of the typical construction profiles with rammed earth as the core, natural stone as the foundation, and fired bricks as the outer masonry wall and wall coping. The interior of the wall consisted only of rammed earth without brick masonry, Shanxi Province (Source: Tongji-ACL)

Fig. 10 Use of lime for construction of the Ming Great Wall. B: Bedding. G: Grouting. P: Pointing (Source: Tongji-ACL)

develop a suitable conservation strategy. Studies of lime mortars and conservation techniques are also funded by the National Natural Science Foundation of China (No. 51978472). Dolomite lime mortars have been reported in the Great Wall north of Beijing (Dettmering et al. 2020; Wang 2021). The use of dolomitic lime is related to the occurrence of dolomitic limestone (Fig. 13).

Based on a preliminary study (Dettmering et al. 2020; Wang 2021) and description of almost aggregate-free lime mortars (Dettmering and Dai 2021), the following advanced analyses with additional methods were carried out on mortars classified in calcium-rich lime or weakly hydraulic and dolomitic limes. Representative samples from previous investigations were selected and analysed

Fig. 11 No other aggregates are visible in dense original joints built in Xinguangwu, Shanxi Province, circa 1374-1575. The largest joint width is approximately 1.5 cm (Source: Tongji-ACL)

Fig. 12 Different stages of restoration during the Ming Dynasty. The largest joint width is approximately 2 cm. Left: earlier Ming Dynasty. Right: later stage (Source: Tongji-ACL)

to obtain deeper insight into the historic background. The aims of this work were first, to investigate harmful salts and to derive their effects on the physico-chemical properties of historic building materials, and second, to develop means to gain knowledge for the future development of compatible lime mortars for sustainable preventive conservations measures at the Great Wall.

3 Investigation objects and methodology

The research study focused on identifying and determining the composition and lime types of masonry mortars from the following sites. The samples were taken and selected in 2019 by the Architectural Conservation Laboratory of Tongji University, Shanghai, in collaboration with the Academy for Heritage Architecture Research of the Beijing University of Civil Engineering and Architecture. The investigated locations marked in green in Fig. 1 refer to the following locations (from east to west):

Suizhong (Liaoning Province), Zunhua, Shanhaiguan (Fig. 15 top), Zhangjiakou (Hebei Province), Badaling, Simatai SMT, Shuiguan, Jiangmaoyu JMY (Fig. 15 bottom) (Beijing), Xinguangwu XGW, Fanshi (Shanxi Province) and Yulin (Shaanxi Province).

In consultation with the project partners, bedding and pointing mortars were selected for the samples (Fig. 14).

During this phase of the investigation, only original older bedding and pointing mortars were examined. However, there are also mortars used in the restoration of the Ming Great Wall that date from more recent times. These differ slightly in colour from the bedding mortars. Such mortars are not the subject of this research.

Combined with material descriptions and sample mappings, the following standard methods of mineralogical and chemical analysis were used to determine whether the binders can be characterised systematically. Approximately 40 samples were selected for chemical-mineralogical analyses. An average of five specimens served as comparative samples of the respective findings.

The samples reported here were selected because they represent the most typical aggregate-free bedding and pointed mortars. With the further analyses presented here for the first time, the special features in the composition are investigated more closely than in the past.

To make an initial assessment of possible damage to the masonry caused by salt loads and possible external influences, selected salt analyses were conducted on samples taken from deteriorated surfaces at several locations (Fig. 15).

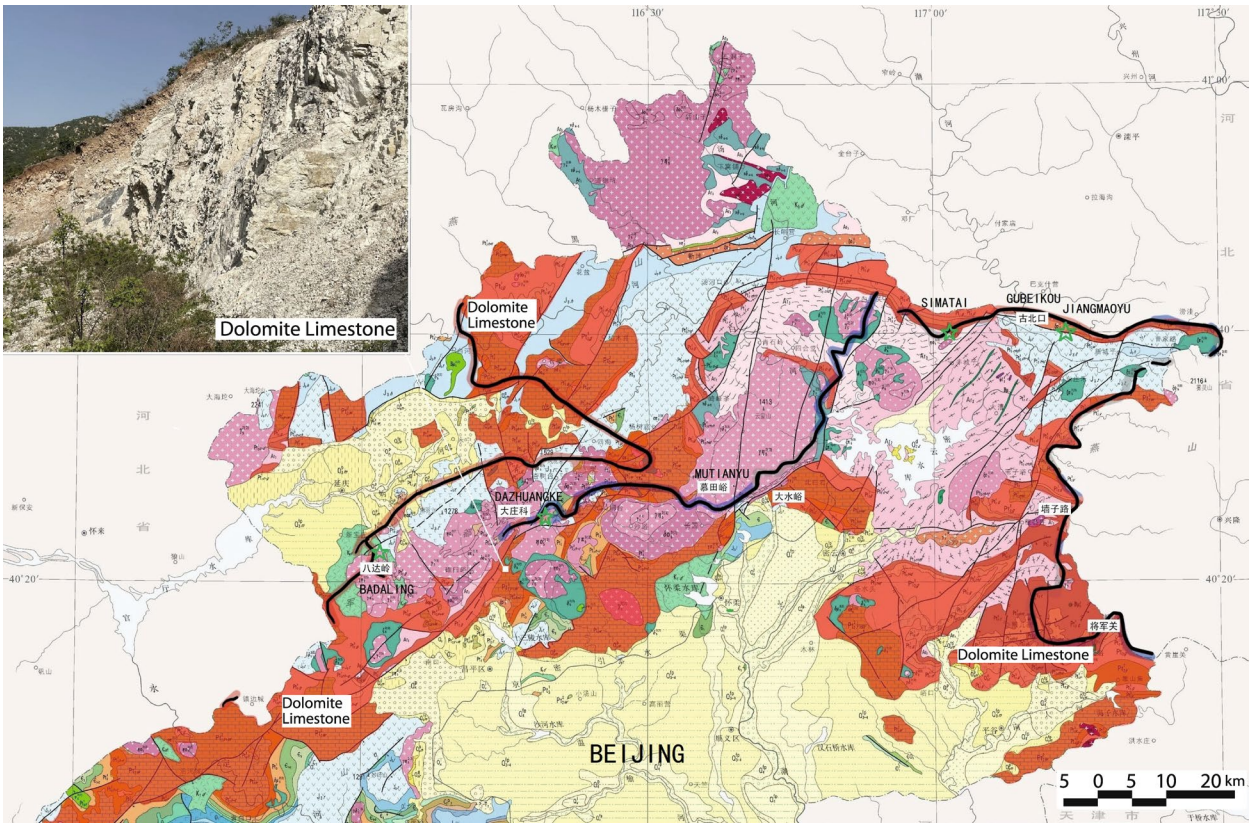

Fig. 13 Location of the Ming Great Wall (simplified) with dolomite limestone occurrences (red orange) (Source: geological map based on http://drr.ikcest.org/map/m02c3?fullscreen=1&gson=#11/39.2065/116.5624)

Fig. 14 Sampling of lime mortars. Left: bedding mortar. Right: pointing mortar from a double struck joint (Source: Tongji-ACL)

3.1 Investigation methods for lime mortars

First, the selected lime mortar samples were described macroscopically in terms of their appearance, colour, texture, and condition. The analytical methodology was carried out according to common standard procedures (Middendorf et al. 2005a; Moropoulou et al. 2004; Elsen 2006). In addition to the mineralogical characterisation of binder components and chemical analyses of aggregate

Fig. 15 Parts of the Ming Great Wall are undergoing heavy efflorescence. Top: Shanhaiguan ruins, Hebei province. Bottom: ruin of a watch tower made of stone brick in Badaling (Source: Tongji-ACL))

materials, it was considered necessary to obtain information for the choice of compatible replacement materials (Middendorf et al. 2005b). One objective was to learn more about the compositions of the binders. Accordingly, criteria were applied to select the appropriate methods. Therefore, broad ranges of techniques used for mineralogical/chemical analysis of historic mortars were considered (Borsoi et al. 2019; Santos et al. 2011; Miriello et al. 2010). For a standard, full chemical-mineralogical analysis, sample quantities of approximately 100 g were necessary. To obtain information about the historic materials as a basis to develop an appropriate repair mortar, thin sections of the mortar samples were prepared. As the results of microscopic examinations of thin sections are often only qualitative, they are not directly applicable to the development of a new mortar with a defined quantitative composition. As an alternative method to the traditional procedures to determine the aggregate grading curve and the binder/aggregate ratio of the historic material, digital image analysis (DIA) has been carried out (Middendorf et al. 2017). Especially in the case of carbonate rock as aggregate, DIA is the only method that can be used to analyse these characteristics of a mortar. Furthermore, DIA was applied to verify the results of the wet-chemical analyses. To compare the equivalent analyses conducted in China and Germany, the traditional methods were given preference, and DIA was used for the advanced analysis of samples.

3.1.1 Chemical-mineralogical investigations

The selected representative samples were analysed by wet-chemistry methods to separate aggregates and binders according to Middendorf et al. (2005b) in reference to Wisser and Knöfel (1987) without destroying the aggregates during the process. Care was taken to detect possible lime-containing aggregates. If preliminary examinations showed that a mortar sample contained acid-insoluble aggregates, the sample was prepared for the determination of soluble silica (CSH phases). The binder content was determined by measuring the difference between the weight of the sample and the weight of the insoluble residue. The carbonate binder was dissolved, and soluble silicates of the hydraulic fraction (if present) were digested. To compare the content of hydraulic phases in historical mortars, the SiO_2 content was related to the measured binder content.

The contents of CaO and MgO were calculated, and the method was specified according to Middendorf et al. (2005a, 2005b, 2005c). For this purpose, atomic absorption analyses of the carbonate binders and qualitative X-ray diffraction (XRD) were performed to determine the phases.

In addition to qualitative X-ray diffraction analysis, quantitative Rietveld X-ray diffraction analysis was applied to characterise their mineral phase constituents in more detail and to analyse their composition in a more differentiated way in the context of wet-chemical analyses and subsequent microscopy.

In all X-ray powder diffractograms, the reflections with the strongest intensity of each phase are referred to by abbreviations. The semi-quantitative evaluation refers to the reflections with maximum intensity of the major and minor phases as well as phases detectable at trace levels. The calculated approximate percentage contents of each phase are included.

Due to the limitations of wet-chemical and X-ray analyses, further polarisation microscopic investigations were carried out on thin sections in combination with scanning electronic analyses. Special attention was given to transformation phenomena during crystallisation.

3.1.2 Microscopic examinations

To obtain further information on the binder type and aggregates, individual samples were examined microscopically.

By using polarised light microscopy, the textural and mineralogical characterisation of the binder phases and aggregates was performed on thin sections. Therefore, bedding and pointing mortars were embedded in epoxy resin by vacuum impregnation and dyed blue to better identify the pore space (Kraus 2015).

The images in the figures show representative sections of the prepared thin sections.

Special attention was given to possible secondary phase formations, reaction zones between binder and aggregate grains, and identification of hydraulic phases.

The thin sections were additionally examined with DIA to analyse the binder/aggregate ratio and the grading curve of the aggregates using an open-source programme ImageJ. In histograms produced by pictures with a magnification of 1:2.5 under plain polarised light, pictures are processed with suitable colour models to a binary image as written in Middendorf et al. (2017). In this case, the binder appears as background (white) and the aggregate and the voids as main objects (black). Binder, aggregate and voids were distinguished by the colour models, filtering out the porosity and calculating with an approximation due to the unknown densities. Careful separation of the aggregate and pores was required. Due to the different types of aggregates, some of which differed only slightly from the binder in the image, manual reworking was necessary by comparing the original image with the binary image, as described in Middendorf et al. (2017).

To gain additional data on the mineralogy and elemental composition of the mortars, select uncovered thin sections were analysed after coating by carbon evaporation by scanning electron microscopy (SEM) coupled with an energy dispersive spectrometer. Scanning electron microscopy was especially used to visualise the surface structures of magnesium-rich lime mortars. A connected energy dispersive X-ray microanalysis (EDX) was used to show element distributions to derive conclusions about possible crystallisation processes.

3.1.3 Investigation of physico-mechanical properties

To obtain information about the physico-mechanical properties, the bulk density and capillary water absorption relevant to building physics were determined. As the light microscope can visualise voids with a size of $>10^{-6}$ m, only a few capillary pores (10^{-5} m – 10^{-8} m) are visible. To obtain reference values for compressive strengths, only some (sufficiently large) specimens were tested. Their ultrasonic velocities were determined to estimate the dynamic elastic modulus.

3.2 Salt analyses

Water-soluble salts were determined at selected sample locations with visible evidence of masonry damage. The salt analyses primarily served to qualitatively identify the types of salts and secondarily allowed the estimation of their quantities. The salt contents of the mortar samples, some of which contained stone fragments, were determined by ion chromatography. For sample preparation, representative subsamples were crushed, dried, homogenised, weighed, filled with cold double-distilled water and eluted for 24 h with shaking; then, the water-soluble ions (sulfate, nitrate, chloride, fluoride, magnesium, calcium, potassium, ammonium, sodium) were determined in the eluate using a two-column ion chromatograph.

4 Initial test results

4.1 Chemical compositions and main components of binders and aggregates

The chemical compositions as well as major and minor components of binders and aggregates of selected mortars are reported in Table 1.

Particularly remarkable is the low content of aggregates common to all mortars (Dettmering et al. 2020; Wang 2021). According to a preliminary study, the lime contents of the original binders range from 67 to 97 wt.%, corresponding to binder-aggregate ratios (B/A ratios) from 1:0.03 to 1:0.33. Compared with the lime mortars of the investigated locations of the preliminary study, the contents of the selected mortars in Table 1 show the lowest B/A ratios in the northern province (Hebei) and medium-low B/A ratios in the western province (Shanxi) at 1:0.18. Similar results for the DIA of the thin sections

Table 1 Chemical-mineralogical components and physical-mechanical values of selected bedding and pointing mortars from the Ming Great Wall

Sample Province Location name	Mortar type	Chemical Composition (Wt.-%)						Component		Aggregate/Grain size distribution		Water absorption		Bulk density	Lime-type
		Orig. binder	B/Aa)	B/Ab)	Hydraul. compon. (binder)	CaO	MgO	Main components	Ancillary components	Main Minerals	Mesh size (mm) through fraction (wt.%)	Wt.-%	Vol%	g/cm3	(DIN-EN*)
Hebei Simatai SMT	bedding mortar	94.68	1: 0.05	1: 0.07	< 0.1	31.73**	20.76 **	$CaCO_3$, $MgCO_3$	$CaCO_3$ (aragonite) SiO_2 (quartz)	quartz	0.063-47% 0.125-72% 0.25-84% 0.5-100%	19.47	33.32	1.72	DL 80-30
Hebei Jiang maoyu JMY	bedding mortar	97.66	1: 0.02	1: 0.05	1.4	30.36	15.52	$CaCO_3$, Mg5(CO3)4(OH)2*4H2O (hy-dromagne-site), MgCO3	$CaCO_3$ (aragonite) SiO_2 (quartz)	quartz, silicates (bricks) feldspars, mica, coal	0.063-68% 0.125-89% 0.25-100%	17.63	29.81	1.69	DL90-30
Shanxi Xinguangwu XGWD	bedding mortar	82.53	1: 0.17	1: 0.19	3.52	49.81	1.06	$CaCO_3$	SiO_2 (quartz) CaSO4·2H2O (gypsum)	quartz, coal	0.063-48% 0.125-66% 0.25-85% 0.5-100%	42.32	48.95	1.16	CL80
Shanxi Xinguangwu XGWF	pointing mortar	81.66	1: 0.18	1: 0.15	5.98	49.39	1.26	$CaCO_3$	$CaCO_3$ (aragonite) Al2SiO5 (cya-nite), SiO_2 (quartz)CSH?	quartz, silicates (bricks) feldspars, mica, coal	0.063-55% 0.125-80% 0.25-93% 0.5-100%	44.58	49.58	1.11	NHL 2/CL80

B/Aa): determined by common combined chemical and mineralogical analytical procedures (Middendorf et al. 2005a, 2005b, 2005c)

B/Ab): determined by Digital Image Analyse (DIA) (Middendorf et al. 2017) based on images of thin sections

*Estimated lime-type based on DIN EN 459-1: 2015-07

**These values were recalculated from almost exclusively available $CaCO_3$ and $MgCO_3$

Source: wet-chemical investigations by CAUP, Tongji University and verified by wet chemical and mineralogical investigations at the University of Kassel and the Institut für Steinkonservierung, Mainz

are comparable to those of the wet-chemical analyses; the deviation is in the range of ±0.03. For modelling, special attention was given to distinguishing between lumps of lime and aggregate, which both may appear black in the DIA histograms. The calcium and magnesium content also varies.

The assumption that the aggregate consists of acid-soluble limestone could be refuted by microscopic examinations. Rather, the binder itself contains relicts of overburned or underburned limestone and is thus also associated with macroscopically observed dense structures. The aggregates consist of mostly quartz and aluminium silicate kyanite (disthene), and very small amounts of mica biotite. There are no indications that limestone and dolomite were added as aggregates. The grain size distributions of the aggregates reflect their high proportion of fine fractions smaller than 0.25 mm (Figs. 18 and 21).

The results show that in some mortars from the northern province of Hebei (near Beijing), relatively high levels of magnesium are present, indicating dolomite in the binder. This particularly true for samples from Zunhua, followed by those from Jiangmaoyu and Zhangjiakou. Regarding the geological map (Fig. 6), the locations at Simatai and Jiangmaoyu are situated at geological deposits of dolomite rock. In contrast, mortars from western Shanxi Province, such as those from Xinguangwu, contain high levels of calcite. Comparable results are also found in mortars from Qianhuangdao (Hebei Province) and in mortars from Suizhong (Liaoning Province), which also indicate calcium-rich limes with very high binder contents and low contents of MgO and hydraulic components. The geological map in Shanxi Province formations is designated marl, mud grey limestones, mixed and micritic limestones and subordinated dolomitic limestones. More detailed investigations of the geological events at the sites, e.g., in the context of relict textures of lime inclusions in the mortars, might provide indicators of provenance for the geological source of the lime binder.

According to European standards and the literature (DIN EN 459-1: 2015-07; Kraus 2016; Dettmering and Kollmann 2019), these limes could be roughly classified into at least three categories (Fig. 16):

- Calcium Lime CL90,
- CL80 and CL70 as well as NHL to
- Dolomitic lime DL90-30, DL90-5 or DL80-30.

The lime types including natural hydraulic lime were estimated because no indication for the appearance of pozzolan or possibly fine proportions of siliceous aggregates developing a pozzolanic effect (Middendorf et al. 2005c) was confirmed by XRD or microscopic investigations.

4.2 Phase constituents according to Rietveld analyses

The analytical results of Rietveld analyses are shown graphically in the figures of the individual diffractograms

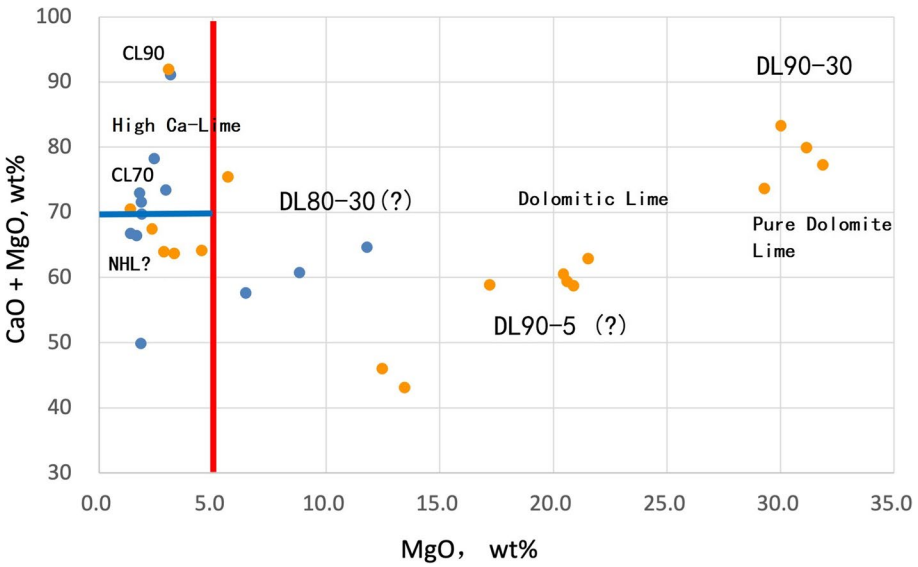

Fig. 16 Main chemical components of lime binders from the Ming Great Wall and estimated types of lime binders (yellow points are samples collected from the Great Wall built by the Ji Town administration, northern provinces, s. Figure 1, blue points are samples from other locations of Ming Great Wall documented in Table 1) (Source: Tongji-ACL)

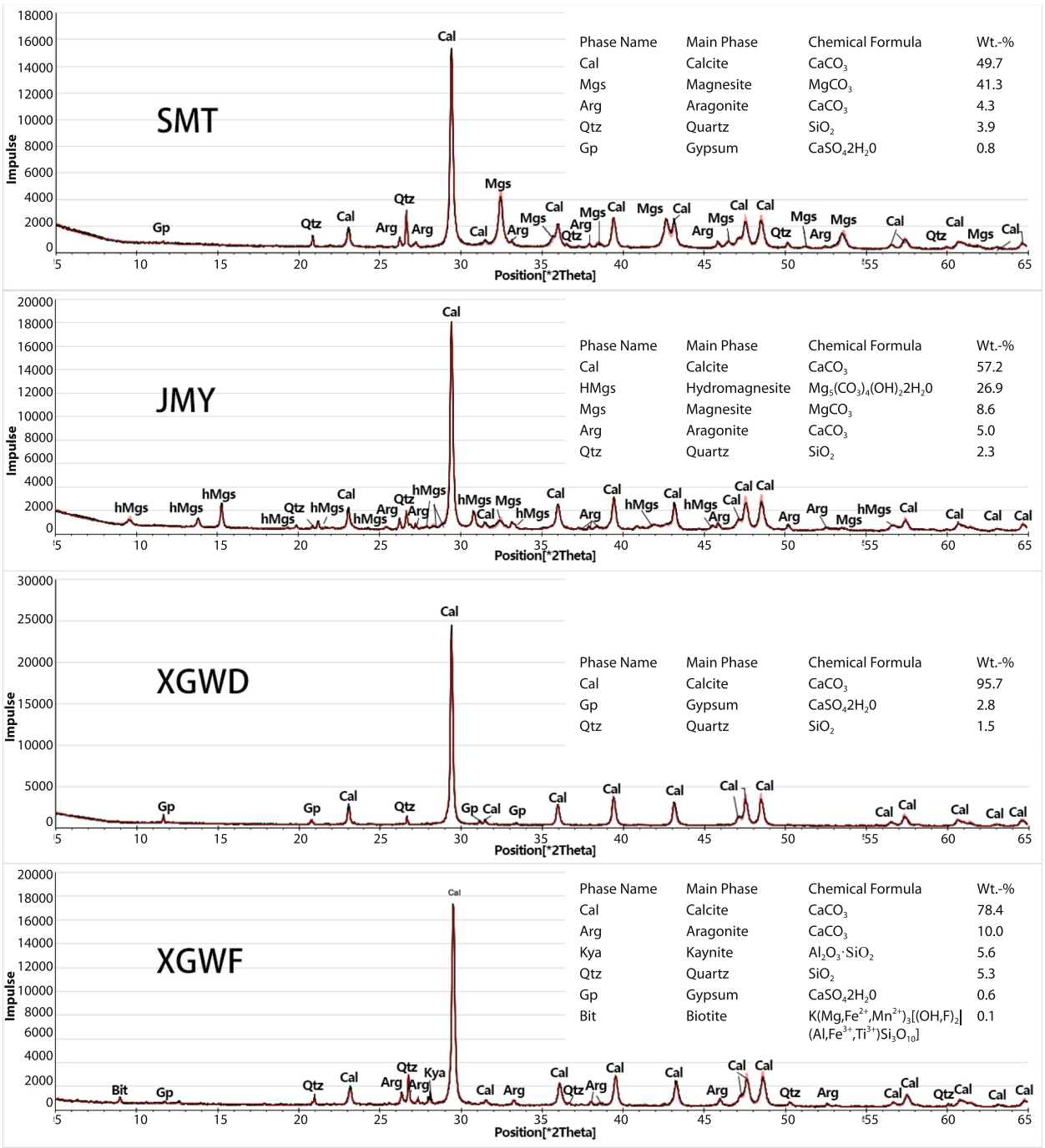

Fig. 17 Diffractograms of the mortar samples JMY (bedding mortar), SMT (bedding mortar), XGWD (bedding mortar), and XGWF (pointing mortar) (Source: Tanja Dettmering and Bernhard Middendorf)

with calculated phase compositions of the lime mortar samples (Fig. 17).

Semiquantitative X-ray diffraction analysis of sample JMY (Fig. 17) according to Rietveld revealed phase constituents of predominantly calcite and hydromagnesite, with magnesite in addition and a small amount of quartz. JMY is therefore categorised as dolomitic lime, now known as DL90-30.

The phase composition of sample SMT showed calcite and magnesite as the main phases. Aragonite was identified as minor phase. In addition, quartz and a small amount of gypsum were detected in the sample.

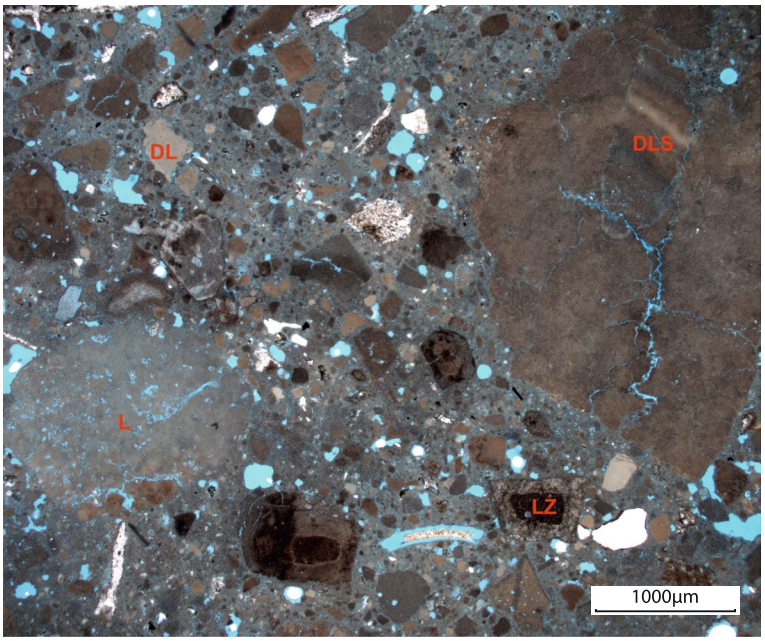

Fig. 18 Microscopic texture of the dolomitic lime mortar from Simatai Beijing showing dense texture in plane-polarised light (ppl). DLS: dolomite limestone relict in a lump of lime. DL: lump of magnesium rich lime. L: lump of lime. LZ: lump of lime inhomogeneous zoned (Source: Tanja Dettmering)

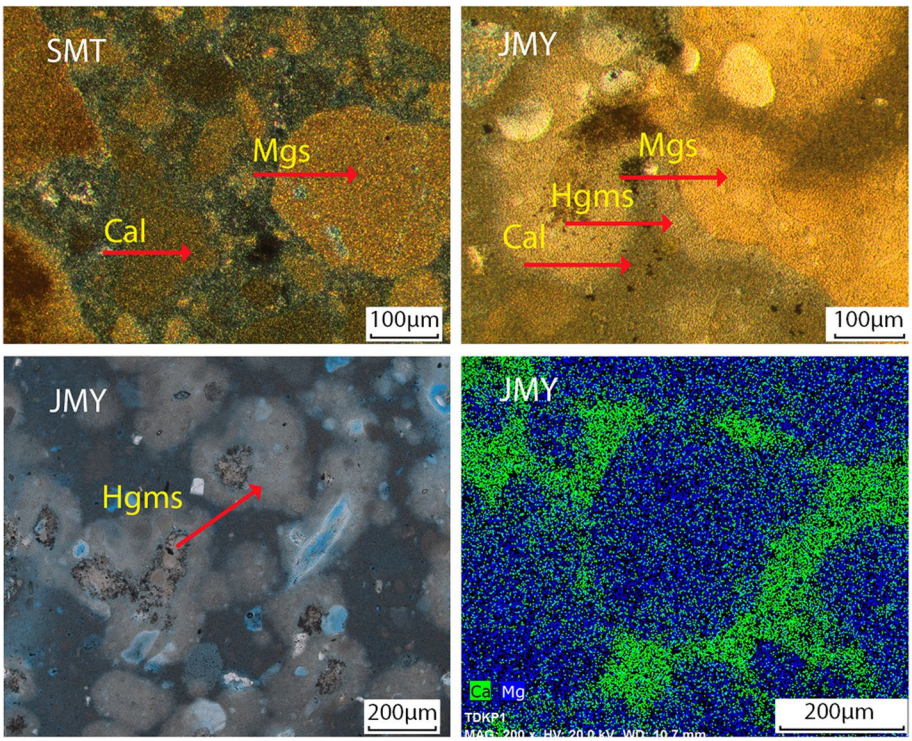

Fig. 19 Representative thin sections of the dolomitic lime mortars SMT Simatai and JMY Jiangmaoyu (top right and bottom) from Beijing. *SMT-top left: bedding mortar with lumps of lime and the indication of dense magnesite (Mgs) and calcite (Cal) in crosspolarised light (xpl). JMY-top right: thin section image of dolomitic lime mortar with the intermediate hydromagnesite (Hgms) of the transformation process to Mgs, Cal or intergranular voids (ppl). JMY- bottom-left: Thin section image of dolomitic lime mortar showing spherulitic carbonate structures and intermediate Hgms in a transition zone (ppl). JMY-right: EDAX image of the Ca- and Mg-enriched regions visible in the thin section.* (Source: Tanja Dettmering and Bernhard Middendorf)

Compared to sample JMY, this sample contained no hydromagnesite but 4.8 times the amount of magnesite. The calcite content was also over 10% higher here, with comparable proportions of aragonite and quartz. Again, a modern classification results in a mortar group DL 90-30.

The phase composition of sample XGWD showed calcite as the main phase. Very small amounts of gypsum and quartz were identified as minor phases. Analogous to the chemical composition, this is a lime mortar, which corresponds approximately to a modern mortar quality CL80.

The phase composition of sample XGWF showed calcite as the main phase. Significant amounts of aragonite were identified as minor phases. Aluminium silicate kyanite (disthene), quartz and, in very small amounts, mica biotite were detected, and small amounts of gypsum were present. The calcium carbonate content in the form of calcite and aragonite determined by Rietveld analysis was lower than that of the previously mentioned sample of this masonry system. Chemical analyses of comparable samples suggest NHL or CL70/80 (Fig. 16).

In some samples of both groups, XRD identified aragonite, which can be seen as an indication of the decomposition of carbonated C-S-H phases with the products of aragonite and silica gel (Diekamp 2014).

4.3 Results of microscopic analyses

4.3.1 Dolomitic lime mortars from Beijing Province using Simatai SMT and Jiangmaoyu JMY as examples

Chemically, both lime mortars have almost the same composition. The average CaO contents of mortar samples from SMT and JMY range from 30 to 31 wt.%, and MgO contents range from 15 to 21%. The binder contents are almost stable, 90–91 wt.%. This also corresponds to today's dolomitic limes DL90-30.

Macroscopically, the bedding mortar SMT has a beige to light brown colour. The carbonated, binder matrix appears brown in PP and brown-grey in XP. Few fine aggregate grains containing quartz are white/grey/black in XP and angular to rounded.

SMT is characterised by a coarse-grained, dense, relatively crack-free compact mortar structure, in which lumps of lime with sizes of approximately 100 µm as well as smaller ones in the range of 20–50 µm are uniformly distributed in the binder matrix (Figs. 18, 19 top left). A small percentage of air-filled pores appear blue in transmitted light. Dolomite limestone relicts (DLS) exist within coarse lime lumps, indicating an underburning process. In addition, light brown lumps of magnesium-rich lime (DL) can also be observed. Some lumps of lime are hardly distinguishable from the binder, slightly lighter in colour and possibly resulting from overburning. Additionally, smaller inhomogeneous, zoned lumps of lime are visible. Quartz grains of maximum size of 30 µm and smaller gypsum grains of a maximum of 20 µm were visible under a microscopically. With a B/A ratio of 1:0.07 determined by DIA, the main fractions < 0.25 mm are almost congruent compared with the wet-chemical analyses; hydromagnesite and spherulitic structures are not visible in the examined SMT samples.

In SMT as well as in JMY, microscopic evidence of a very dense, crack-free microstructure due to post-slaking periclase (MgO) is found.

JMY represents bedding and pointing mortar in a composite of brick and granite masonry. It has a light beige to light grey colour with a dense and crack-free binder structure. A small percentage of pores appear blue in transmitted light. The carbonated dolomitic lime appears beige-brown in PP (Fig. 19 top right) and brown-grey in XP (Fig. 19 bottom left). Darker than white lime in PP and XP, the binder matrix shows spherulitic, partly heterogeneous and delineated dense sections of Mg-H-CO_3 phases. Few fine aggregate grains containing quartz are visible, white/grey/black in XP, from angular to rounded. The B/A ratio of 1:0.05, determined by DIA, with main fractions < 0.125 mm, is almost congruent compared to the results of the wet-chemical analyses. The lumps of lime are distributed, varying in size in the 50–150 µm range with some larger particles up to two mm. Since the semiquantitative X-ray diffraction determined by Rietveld identified predominantly calcite, hydromagnesite and magnesite as phase components, these minerals are assumed to be finely crystalline in the matrix and lime lumps.

All thin section micrographs of the dolomitic lime mortar of JMY show spherulitic carbonate structures (Fig. 19) and a transition area caused by crystallisation processes. This suggests that separate carbonation of Ca and Mg phases is involved.

The spherulites represent accumulations of much smaller crystals. They are formed preferentially at crystallisation nuclei and grow uniformly in all directions from their centres, forming spherical, radially symmetric arrangements. Growth occurs if they are surrounded by amorphous material.

The SEM/EDAX images examined in these areas (Fig. 19, bottom right) show a clear separation of Ca- and Mg-containing areas. Here, Mg is concentrated in the cores of lime lumps. According to recent findings by Diekamp (2014), it can be assumed that aggregates of hydromagnesite crystals with spherulitic structures form around crystallisation nuclei. Hydromagnesite occurs as an intermediate in a kinetically delayed setting process from brucite to magnesite. The voids are filled with calcite, the solidification

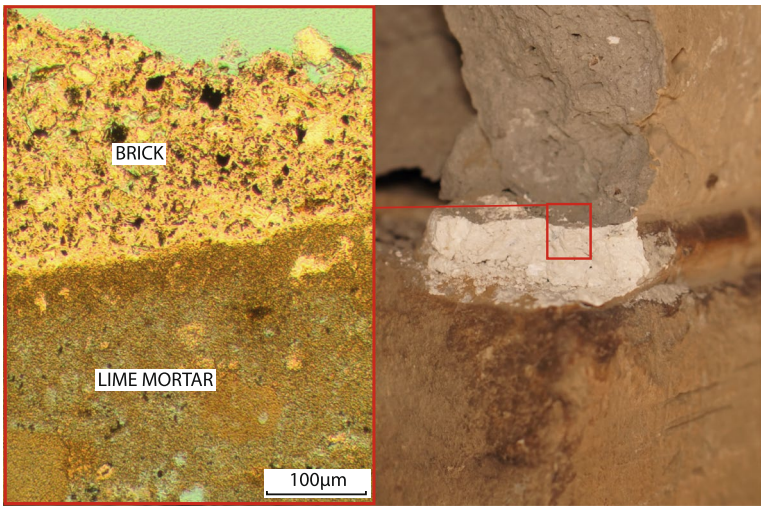

Fig. 20 Macro- and micro-scale texture of the bedding and pointing mortar in Xinguangwu. Joint width is approximately 1.0 cm (Source: Tanja Dettmering and Tongji-ACL)

product of the calcium phase, in a fine-grained matrix. Thus, a dense and stable crystal structure is formed.

4.3.2 Lime mortars with varying hydraulic contents from Shanxi Province using the example of Xinguangwu (XGW)

Samples XGWD and XGWF were taken from different parts of the wall from Xinguangwu (XGW) in western Shanxi Province. XGWD originates from the bedding mortar of the passageway of a weapon tower built of bricks. The average CaO contents of the comparative samples in the 50——53 wt.% range, and the MgO contents are less than 2 wt.%. The binder contents vary between 69 and 82 wt.% (Dettmering et al. 2020; Wang 2021). Based on comparable samples with hydraulic components from 3.5 to 7 (wt.%), the lime binders of XGW could be classified as NHL or CL80.

XGWD and XGWF both have white-beige fine macrostructure (Fig. 20, right).

The microscopic thin section shows very good bonding between lime mortar and the old brick stone (Fig. 20, left).

In the thin sections, no magnesite is found in those samples (Fig. 17). In transmitted light, the mortar matrix of both bedding and pointing mortars appears as a fine, homogeneous microstructure with predominantly smaller lumps of lime (50–150 µm), aggregates of quartz (approximately 50 µm), silicate fragments and isolated charcoal inclusions in the 10–20 µm size range uniformly distributed in the binder matrix (Figs. 21 and 22). A small percentage of air-filled pores appear blue in transmitted light. With B/A ratios of 1: 0.15–0.19, determined by DIA, and with main fractions < 0.25 mm, the results are almost congruent compared with those of the wet-chemical analyses.

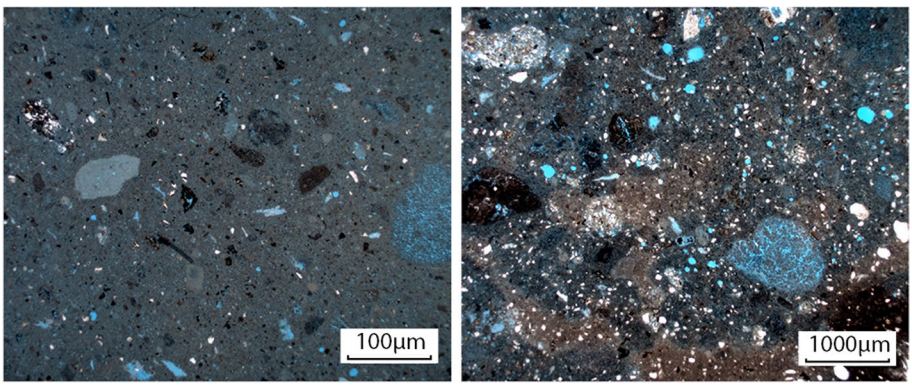

Fig. 21 Mortar matrix of the bedding (left) and pointing (right) mortars from XGW (xpl) (Source: Tanja Dettmering)

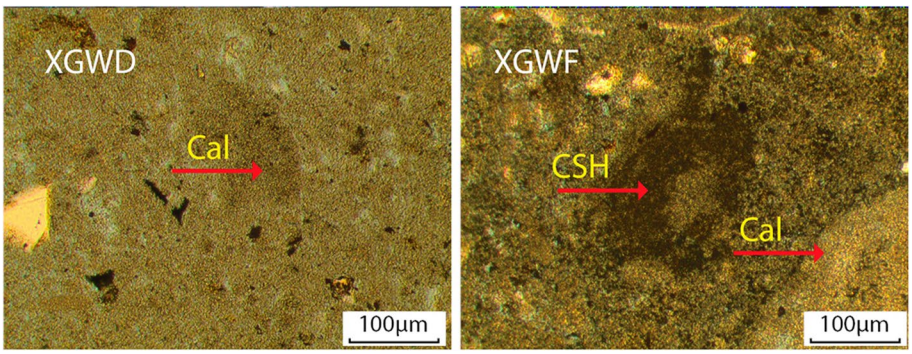

Fig. 22 Microstructure of calcium-rich lime mortar (All ppl). Left: bedding mortar consisting of a dense mortar matrix as a fine, homogeneous microstructure with predominantly smaller lime patches. Right: pointing mortar with lumps of lime covered by fine crystalline cloud-like structures, indicating the CSH phase (Source: Tanja Dettmering and Bernhard Middendorf)

Larger lime (calcite) lumps on the order of 150–200 µm appear to be covered by cloud-like structures typical of CSH phases. They often have fine crystalline structure and cannot be resolved with a light microscope but can be described as "clouds" (Goedeke and Goretzki 2007; Válek et al. 2012; Kraus 2015).

4.4 Investigation of physico-mechanical properties

The results of bulk densities and capillary water absorption from selected mortars are reported in Table 1. The bulk densities of approximately 1.7 g/cm^3 are in the range of unpublished values of bulk densities of typical dolomitic lime mortars from Beijing with measured maximum values of 1.8 g/cm^3. Compared with those mortars, SMT and JMY correspond to low porosities with values of approximately 18% by weight and 30% by volume. Ultrasonic velocities of 800 m/s and comparatively high compressive strengths > 7 MPa were measured on individual samples.

The XGW lime mortars based on calcium-rich lime binders show lower bulk densities ranging between 1.1 and 1.2 g/cm^3. They are more porous than dolomitic lime mortars, and the capillary porosities of calcium-rich lime mortars are on average 45% by volume and 50% by volume. These values also correspond exactly to the unpublished results of the previously examined larger series of mortars of calcium-rich lime binders of the Great Wall. Compressive strengths of comparative samples could be measured > 6 MPa, lower than those of dolomitic lime mortars, but still relatively high for lime mortars with very low levels of hydraulic components.

4.5 Results of salt analyses and observed damage

The results for water-soluble salts from selected sample sites are shown in Table 2.

High levels of magnesium sulfates and chlorides were found, especially in the efflorescence. In a sample of the masonry surface consisting of bricks and dolomitic lime mortar from Shanhaiguan (see Fig. 15), Mg and SO_4 ions up to > 50 wt.% were determined.

Dolomitic lime mortars containing abundant magnesium under appropriate conditions can serve as a source of magnesium. The high values can be explained by the concentration of salts on the surface due to high evaporation rates.

5 Interpretation of the results and assessment

5.1 Types of lime binders

The investigation results show that bedding and pointing mortars are composed of predominantly dolomitic calcium-air lime binders and a few mortars with natural

Table 2 Water-soluble salts from Shanhaiguan/Hebei and Badaling/Beijing (wt.%)

Location	Sample	Na^+	NH_4^+	K^+	Ca^{2+}	Mg^{2+}	F^-	Cl^-	NO_3^-	SO_4^{2-}
Hebei, Shanhaiguan/September 2019	H-SHG-Y01	NN	0.33	0.43	1.00	12.65	NN	3.65	NN	59.65
	H-SHG-Y02	0.19	0.09	0.42	1.64	6.76	≤0.01	7.75	0.30	30.42
Beijing, Badalin/October 2020	BDL-03	0.14	–	–	0.31	0.9	–	0.18	0.46	6.84
	BDL-04	0.02	–	–	0.02	0.31	–	0.12	0.17	1.41

NN not detectable, – not analysed

hydraulically reactive binders. Both dolomitic limes and lime mortars rich in calcium are mixed without or with small amounts of aggregates. They consist almost exclusively of binder and fine aggregates. As investigated in more detail in this report, the detected lumps of lime are caused by the use of coarse-grained lime and can occur during the dry slaking process. They can act as lime reservoirs in the binder and/or as aggregates. The dolomite detected by radiography could be an indication of simultaneous use as a binder and as an aggregate or weakburning.

5.1.1 Dolomitic lime binders

For the construction of the Great Wall around Beijing, in Zunhua, east of Beijing, lime mortars consisting of approximately 5–22 wt.% MgO were used (Dettmering and Dai 2021; Wang 2021). Based on chemical analyses, they can be classified as dolomitic limes according to modern lime classification.

Particularly dense microstructures and high compressive strengths at specific points can be measured on mortars made from dolomitic limestones, which are not described in more detail here.

The starting material for dolomitic lime mortars is dolomite or dolomitised limestone, which is widespread in the vicinity of the examined wall. During firing, CaO and MgO are formed, hydrating during slaking to form portlandite or $Ca(OH)_2$ and brucite or $Mg(OH)_2$. The Ca- and Mg- contents were independent of each other and change at different rates during slaking.

In addition to the carbonate phases (calcite and magnesite), which are dominant in dolomitic lime mortars, hydromagnesite indicates lime mortars with relatively high proportions of magnesium. Hydromagnesite is a typical phase formed from brucite $Mg(OH)_2$ during the setting process of slaked dolomitic lime, which slowly reacts to form magnesite. Microscopic examination results support this thesis. Microscopic proof for clearly separated Ca- and Mg-enriched phases indicate crystallisation process that proceeded separately. According to Diekamp (2014), the crystallisation processes typical of dolomitic lime mortar occurring at different rates can be explained by the reaction of $Mg(OH)_2$ and CO_2 to form $MgCO_3$ (magnesite) and H_2O. This process proceeds very slowly and via various intermediate phases, such as the formation of hydromagnesite. This hardening reaction depends on the general conditions during the setting process of the mortar (moisture content in the mortar, CO_2 and moisture content of the surrounding atmosphere). Due to the kinetic delay, the carbonation of brucite to magnesite proceeds more slowly than the carbonation of $Ca(OH)_2$ to $CaCO_3$. The process of slow formation of stable magnesite takes place over very long periods of time and in some cases is not yet complete even after several centuries (Siedel and Laue 2003; Diekamp 2014). The dense microstructures of the dolomitic lime mortars can be explained by crystallisation processes.

In addition to hydromagnesite, nesquehonite and an X-ray amorphous phase are described as further intermediate stages. To what extent these can be explained by transformation processes influenced by fire and slaking processes can only be assumed at the present time.

5.1.2 Calcium-rich lime and lime with weak hydraulic components

In contrast to the occurrence of dolomitic lime mortars, calcium-rich limes dominate in the western province of Shanxi in Xinguangwu (XGW). Due to the geology and appearance of the limestones, both massive pure and clayey limestones were used for the construction of the Xinguangwu wall, which runs over three mountain passes, so it can be assumed that limestones with different levels of impurities were used for the production of lime binders.

The predominantly submicroscopic hydraulic phases present in the natural binders due to the comparatively low firing temperatures are typical for historic mortars (Gödicke-Dettmering 1996; Hughes et al. 2009; Bader et al. 2020). Aragonite, as a product alongside silica gel, provides a further indication of the decay of carbonated CSH phases, which cannot be directly identified by XRD due to their amorphous structure (Diekamp 2014). The geological source of the lime binder at the sites in context with local occurrences of marl has not yet been clarified and requires thorough investigations of textures in mortars and limestones.

5.1.3 Ratio of lime binders and aggregates

Although mortars with lime binders and a high percentage of sand were found at a few sites, the bedding and pointing mortars investigated contained low percentages of aggregates. The present results seem to agree with research by (Dai et al. 2016; Dai 2018). In the so-called method of wind-slaking inherited from China, burnt lime was slaked with little moisture by slowly blowing it into powder in humid air. According to this production method described from the Northern Song to the end of the Ming Dynasty, relatively high strengths could be achieved with the lime produced by this method. No aggregates are mixed to such slaked building lime.

Despite high binder contents, no shrinkage cracks could be detected on the samples. Instead, mainly limestone relicts, partly over— or underburned lime putties and a small number of aggregates are embedded in a homogeneous crystalline binder matrix.

5.2 Possible causes of damage due to reactions between binder and particles as a result of air pollution

The presence of magnesium sulfates on masonry surfaces correlates with dolomitic lime mortars, as observed in Europe (Siedel and Laue 2003).

These sulfates are formed as characteristic reaction products under the influence of sulfur dioxide during specific climatic stresses. Depending on the moisture situation in the masonry, different effects and types of damage can be observed.

Until a few years ago, SO_2 pollution in correlation with coal consumption played a special role in natural stone weathering in China, especially prior to mandatory flue gas desulfurisation. In the years between 2000 and 2014, coal consumption almost tripled to 1.96 billion tonnes, which was more than half of global consumption (Rasch 2015). Today, a reversal in the trend of carbon dioxide emissions from fossil fuels is noticeable.

6 Conservation strategies for restoration of lime mortars based on new findings

In 2019, it was officially declared that the Ming Great Wall shall be preserved as a ruin. Following the new principles and guidelines, repointing, grouting and partial rebuilding to the Wall head shall be applied to preserve the historic construction in situ. Lime must be used as a binder for all kinds of mortars, with no distinction made between lime types.

Although dolomitic lime performed remarkably well during the construction period of the Ming Great Wall, it is not recommended as a binder for restoration mortars. One reason is that there are no manufacturers or technicians who can handle dolomitic building lime. Another argument is the durability of dolomitic lime under present conditions of air pollution. Calcium-rich lime such as CL90 could be more suitable as a binder for bedding and repointing mortars. Due to its very slow carbonation in built masonries and its associated low strength and low resistance to frost, calcium-rich lime such as CL90 without pozzolanic addition is not recommended for structural consolidation (Historic England 2012 and 2017). International studies on dolomitic lime have shown that high sulfate-resistant hydraulic binders are preferred for structural conservation. An alternative might be formulated lime, i.e., high calcium lime gauged with natural pozzolan.

Basic principles must be applied to the use of lime. The strength and modulus of elasticity of the mortars should be less than the values of the bricks. In addition to physical requirements, special attention should be given to the quality of modern lime. The air lime available in China today is either slaked on site or finely ground in factories. Its unchanged application without aggregates for bricklaying or filling would cause damage such as shrinkage or weak bonding to bricks and stones. Today, there are also approaches to restoration with high proportions of lime in binders; however, difficulties and damage have occurred as the result of this approach. One reason for this is that at the present time, limes are fired at higher temperatures and over a shorter period than they were in the past. Additionally, in the last, limes were not tested according to current building lime standards, which would allow comparisons to be made. New experiments and the optimisation of lime mortars might be necessary to avoid new damage to historic structures.

The compatibility between new mortars and historically contaminated structures should also be considered to avoid damage to the masonry (Auras et al. 2010).

In the case of high levels of salt contamination, desalination with the use of sacrificial plasters based on local soils and lime prior to conservation intervention should be tested to improve the durability of the conservation measurements.

For earthworks, both air lime and natural hydraulic lime can be used to consolidate earth, but their suitability should be tested for resistance to frost damage under extremely dry climates and with short working times (Kuhl 2019).

7 Conclusions and discussion

The present test results confirm that lime used for construction of the Ming Great Wall ranged from pure dolomitic lime to pure calcitic lime. Calcium air limes with few natural hydraulically reactive binder phases were also found. The lime bedding and pointing mortars from the Ming Great Wall were characterised by high contents of lime binder, with or without small amounts of aggregate.

In dolomitic lime mortars, particularly dense microstructures and high strengths were observed, which contributed to the good state of preservation of the Great Wall in the regions of Hebei and Beijing. However, soluble magnesium sulfate hydrates in addition to chlorite and nitrate were observed.

Calcium lime was widely used as a binder for bedding and pointing mortars. Even in regions where geologic deposits of dolomite limestone and calcium limestone deposits occur, e.g., Xinguangwu, calcium limestone was preferably used to produce lime.

The extent to which lime with hydraulic components was used, depending on regional deposits, has not yet been clarified. One clue is provided by aragonite as a

decay product of carbonated CSH phases, which cannot be directly identified by XRD due to their amorphous structure. More precise indications can be provided by further investigations using differential thermal analysis/thermogravimetric analysis (DTA/TG), Fourier transform infrared spectroscopy (FTIR) and attenuated total reflection infrared spectroscopy (ATR-IR).

A new lime system should be designed according to authenticity, technical considerations, economic feasibility and priorities of modern administration to conserve the masonry ruins of the Ming Great Wall. Dolomitic lime is rather unsuitable for conservation measures under present climatic conditions. For the given reasons, natural hydraulic lime or pozzolan-modified lime with high calcium contents are currently more functional types of conservation binders for preserving the ruins of the Great Wall.

Abbreviations

Cal: Magnesium calcite (magnesite); Hmgs: Hydromagnesite, the finest-grained, partly amorphous (according to X-ray analysis), partly hydrous or basic magnesium carbonates formed after hardening and carbonation of dolomitic lime; CSH: Calcium silicate hydrate phases, the finest-grained, partly amorphous (according to X-ray analysis), calcium silicate hydrate and calcium aluminate hydrate phases formed during pozzolanic and hydraulic hardening; XRD: X-ray diffraction; EDX: Energy-dispersive X-ray spectroscopy; SEM: Scanning electron microscopy; FTIR: Fourier transform infrared spectroscopy; ATR-IR: Attenuated total reflection infrared spectroscopy; ppl: Plane-polarised light; Tongji-ACL: Architectural Conservation Laboratory of Tongji University.

Acknowledgements

Professor Yuyang Tang and Dr. Zhaoyi Liu of the Academy for Heritage Architecture Research at Beijing University of Architecture and Civil Engineering, Tao Zhang of Beijing Institute of Ancient Heritage Architecture, Mr. Bo Li of Beijing Construction for Ancient Architecture are thanked for their cooperation as well as Zhanyong Hu, Yijie Wang, Yuee Zhou & Faling Ju of the Architectural Conservation Laboratory of Tongji University, Shanghai. Our special thanks go to Prof. Dr. Bernhard Middendorf of the University of Kassel, who gave us the opportunity to collaborate on microscopic and XRD Rietveld analyses. We would like to expressively thank Dr. Karin Kraus and Dr. Michael Auras from the Institut für Steinkonservierung e. V. in Mainz, Germany, for their numerous suggestions and everlasting willingness to discuss. We also like to thank for their explicit consent and interest in the publication of the study in English, which was presented during the online-colloquium in April, 2021 in Germany by Dettmering & Dai.

Authors' contributions

The authors read and approved the final manuscript.

Funding

The research project was initiated by the China National Cultural Heritage Administration and supported by the National Natural Science Foundation of China (No. 51978472 & 51738008) and the Open Projects Fund (No. 2019010109) of Tongji University, as well as the project "Technical Guideline for the Conservation of Stone Masonry of the Ming Great Wall " of the China National Cultural Heritage Administration.

Availability of data and materials

Not applicable.

Declarations

Competing interests

The authors declare that they have no competing interests.

Author details

[1]August-Bebel-College, Richard-Wagner-Straße 45, 63069 Offenbach, Germany. [2]Architectural Conservation Laboratory CAUP Tongji University, No. 1239 Siping Road, Shanghai 200092, China.

Received: 12 July 2021 Accepted: 8 January 2022
Published online: 02 February 2022

References

Auras, Michael, Jeannine Meinhardt, and Rolf Snethlage. 2010. *Leitfaden Naturstein-Monitoring - Nachkontrolle und Wartung als zukunftsweisende Erhaltungsstrategien*. Stuttgart: Fraunhofer IRB Verlag.

Bader, Tobias, Judith Gagl, and Anja Diekamp. 2020. "Dolomia: A Survey on the historic and present-day use of dolomite rock as building material in tyrol." In *Proceedings of the 14th international Congress on the Deterioration and Conservation of Stone, Monument Future Decay and Conservation of Stone*, edited by Siegfried Siegesmund and Bernhard Middendorf, 1071–1076. Mitteldeutscher Verlag.

Borsoi, Giovanni, Santos Silva, Menezes António, P. Candeias, António Jose, and José Mirao. 2019. "Analytical characterization of ancient mortars from the archaeological roman site of Pisões (Beja, Portugal)." *Construction and Building Materials* 204: 597–608 http://www.elsevier.com/locate/conbuildmat.

Dai, Shibing. 2018. "Preliminary study on wind slaked lime used before Qing dynasty in China." *Journal of Architectural Conservation* 24 (2): 91–104.

Dai, Shibing, Yan Zhong, and Zhanyong Hu. 2016. *Ten questions on lime work - lime Technology for Built Heritage Conservation*. Shanghai: Tongji University Press.

Dettmering, Tanja, and Shibing Dai. 2021. "Mörtel aus der chinesischen Ming-Großmauer - erste Analysenergebnisse und Beschreibung der Kalkarten." In *Wissenschaftliches Kolloquium zu Kalkmörteln, —putzen und –farben anlässlich des 30ig-jährigen Bestehens des Instituts für Steinkonservierung e. V., IFS-Bericht Nr. 62, edited by Alles Kalk*, 61-80.

Dettmering, Tanja, and Helmut Kollmann. 2019. *Putze in Bausanierung und Denkmalpflege, 3. überarbeitete Auflage*. Berlin: Beuth-Verlag.

Dettmering, Tanja, Zhaoyi Liu, Yuyang Tang, Yijie Wang, and Shibing Dai. 2020. "Preliminary study on lime mortars used for stone masonry of the Great Wall built by Ming Dynasty in China." In *Proceedings of the 14th international Congress on the Deterioration and Conservation of Stone, Monument Future Decay and Conservation of Stone,* edited by Siegfried Siegesmund and Bernhard Middendorf, 793-798. Mitteldeutscher Verlag.

Diekamp, Anja. 2014. "Bindemitteluntersuchungen an historischen Putzen und Mörteln aus Tirol und Südtirol." PhD diss., Leopold-Franzens-Universität Innsbruck.

DIN EN 459-1. 2015-07. *Baukalk – Teil 1: Begriffe, Anforderungen und Konformitätskriterien*. Berlin: Beuth Verlag.

Elsen, Jan. 2006. "Microscopy of historic mortars – A review." *Cement and Concrete Research* 2006 (36): 1416–1424. https://doi.org/10.1016/j.cemconres.2005.12.006.

Forster, Alan M. 2010. "Building conservation philosophy for masonry repair: Part 2 - 'principles'." *Structural Survey* 28: 17 f.

Gödicke-Dettmering, T. 1996. "Mineralogische und technologische Eigenschaften von hydraulischem Kalk als Bindemittel von Restaurierungsmörteln für Baudenkmäler aus Naturstein." PhD diss., Justus-Liebig-Universität Gießen.

Goedeke, Holle, and Lothar Goretzki. 2007. Neue Erkenntnisse zu den Eigenschaften von NHL-gebundenen Mörteln. IFS-Bericht Nr 26: S.14–S.23.

Historic England. 2008. *Conservation principles, policies and guidance. English Heritage,1 London*. https://historicengland.org.uk/images-books/publications/conservation-principles-sustainable-management-historic-environment/conservationprinciplespoliciesandguidanceapril08web/.

Historic England. 2012. *Practical building conservation stone*.

Historic England. 2017. *Repointing brick and stone walls guidelines for best practice.* https://historicengland.org.uk/images-books/publications/repointing-brick-and-stone-walls/.
Hughes, David C., D. Jaglin, Roman Kozłowski, and D. Mucha. 2009. Roman cements – Belite cements calcined at low temperature. *Cement and Concrete Research* 39 (2): 77–89.
Kraus, Karin. 2015. *Historische Mörtel im Dünnschliff, IFS-Bericht Nr. 48.* Mainz: Institut für Steinkonservierung e.V.
Kraus, Karin. 2016. *Kalk - Bindemittel für Farben und Mörtel. Teil 3: Kalkarten. Themenbereich 1.1. Johannesberger Arbeitsblätter, Hrsg.* Fulda: Beratungsstelle für Handwerk und Denkmalpflege Propstei Johannesberg.
Kuhl, Oliver. 2019. "Basic principles for soil treatment with binder – Stabilization of fine-grained soil with lime." Paper presented at the Joint Annual Meeting & International Conference on ICOMOS -CIAV&ISCEAH, Vernacular & Earthen Architecture towards Local Development, Pingyao, September 6–8.
Li, Li, Linyi Zhao, and Mouxiong Li. 2014. "Study on the physical and mechanical properties of several lime materials in ancient Chinese architecture." *Science of Conservation and Archaeology* 3: 74–84.
Luo, Zewen, Wenbao Dai, and Wilson Dick. 1993. *Die Große Mauer - Geschichte, Kultur- und Sozialgeschichte Chinas.* Augsburg: Weltbild Verlag.
Middendorf, Bernhard, John J. Hughes, K. Callebaut, G. Baronio, and Ioanna Papayianni. 2005a. "Investigative methods for the characterization of historic mortars. Part 1: MineralogicalCharacterization." *Materials and Structures* 38: 771–780.
Middendorf, Bernhard, John J. Hughes, K. Callebaut, G. Baronio, and Ioanna Papayianni. 2005b. "Investigative methods for the characterization of historic mortars. Part 2: Chemical characterization." *Materials and Structures* 38: 761–769.
Middendorf, Bernhard, Karin Kraus, and Christina Ott. 2005c. "Influence of the fines of natural sands as pozzolanic components on the interpretation of the acid soluble silica content of historic lime mortars." In *Proceedings of the International Building Lime Symposium,* edited by R.C. Jaffe, Orlando, March 9–11.
Middendorf, Bernhard, Tim Schade, and Karin Kraus. 2017. "Quantitative analysis of historic mortars by digital image analysis of thin sections." *Restoration of Buildings and Monuments.* 23 (2): 83–92. https://doi.org/10.1515/rbm-2016-0011.
Miriello, Domenico, Donatella Barca, Andrea Bloise, Annamaria Ciarallo, Gino M. Crisci, De Rose Teresa, et al. 2010. "Characterisation of archaeological mortars from Pompeii (Campania, Italy) and identification of construction phases by compositional data analysis." *Journal of Archaeological Science* 37: 2207–2223. https://doi.org/10.1016/j.jas.2010.03.019.
Moropoulou, Antonia, Asterios Bakolas, and Eleni Aggelakopoulou. 2004. "Evaluation of pozzolanic activity of natural and artificial pozzolans by thermal analysis." *Thermochimica Acta* 420: 135–140.
Rasch, Jonas. 2015. "Under the dome – Chinas langer Weg zu sauberer Luft." *Argumente und Materialien in der Entwicklungszuammenarbeit* 16: 7-15. https://www.hss.de/download/publications/AMEZ_16_Klimawandel_02.pdf.
Santos, Silva, Cruz Antonio, T. Paiva, M.J. Candeias, Adriano Antonio, Schiavon Patricia, Mirão Nick, and A.P. José. 2011. "Mineralogical and chemical characterization of historical mortars from military fortifications in Lisbon harbour (Portugal), Environ." *Earth Science* 63: 1641–1650.
Siedel, Heiner, and Steffen Laue. 2003. "Herkunft, Kristallisation und Hydratstufenwechsel von Magnesiumverbindungen im Kalkmörtel." In *Umweltbedingte Gebäudeschäden an Denkmälern durch die Verwendung von Dolomitkalkmörteln*, Institut für Steinkonservierung e.V., 31–38. Mainz: IFS-Bericht Nr. 16.
Válek, Jan, John J. Hughes, and Caspar J.W.P. Groot. 2012. *Historic Mortars: Characterisation, Assessment and Repair.* RILEM Bookseries Vol 7. Dordrecht: Springer.
Wang, Yijie. 2021. "Preliminary study on problems of in-situ preservation of the Great Wall built with dolomitic lime." Master's thesis. Tongji University.
WHC World Heritage Committee. 2018. *The Great Wall. State of Conservation Report.* https://whc.unesco.org/en/sessions/43com/documents/#state_of_conservation_reports.
WHC World Heritage Committee. 2019. *The Great Wall. State of Conservation Report.* https://whc.unesco.org/en/soc/3945.
Wisser, Stefan, and Dietbert Knöfel. 1987. "Untersuchungen an historischen Putz- u. Mauermörteln. T.1 Analysengang." *Bautenschutz und Bausanierung.* 10: 124–126.
Yang, Fuwei, Bingjian Zhang, and Qinglin Ma. 2010. "Study of Sticky Rice-Lime Mortar Technology for the Restoration of Historical Masonry Construction." *Accounts of Chemical Research* 43 (6): 936-944. https://doi.org/10.1021/ar9001944.

Publisher's Note

Springer Nature remains neutral with regard to jurisdictional claims in published maps and institutional affiliations.

Submit your manuscript to a SpringerOpen journal and benefit from:

- ► Convenient online submission
- ► Rigorous peer review
- ► Open access: articles freely available online
- ► High visibility within the field
- ► Retaining the copyright to your article

Submit your next manuscript at ► springeropen.com